Droplet impact on regular micro-grooved surfaces*

Hu Hai-Bao(胡海豹)†, Huang Su-He(黄苏和), and Chen Li-Bin(陈立斌)

College of Marine, Northwestern Polytechnical University, Xi'an 710072, *China*

(Received 19 January 2013; revised manuscript received 20 April 2013)

We have investigated experimentally the process of a droplet impact on a regular micro-grooved surface. The target surfaces are patterned such that micro-scale spokes radiate from the center, concentric circles, and parallel lines on the polishing copper plate, using Quasi-LIGA molding technology. The dynamic behavior of water droplets impacting on these structured surfaces is examined using a high-speed camera, including the drop impact processes, the maximum spreading diameters, and the lengths and numbers of fingers at different values of Weber number. Experimental results validate that the spreading processes are arrested on all target surfaces at low velocity. Also, the experimental results at higher impact velocity demonstrate that the spreading process is conducted on the surface parallel to the micro-grooves, but is arrested in the direction perpendicular to the micro-grooves. Besides, the lengths of fingers increase observably, even when they are ejected out as tiny droplets along the groove direction, at the same time the drop recoil velocity is reduced by micro-grooves which are parallel to the spreading direction, but not by micro-grooves which are vertical to the spreading direction.

Keywords: micro-groove, droplet, drop impact, spreading, fingers

PACS: 47.55.Dz, 47.54.De, 61.30.Pq **DOI:** 10.1088/1674-1056/22/8/084702

1. Introduction

A droplet impact on solid surface is a normal phenomenon which exists widely in nature, traffic, new energy, fields of aviation, and spaceflight, and so on. The phenomenon has been discussed for 100 years.[1] However, as the phenomenon is very fast (on the order of a few milliseconds), the early study is not accurate.[2,3] Thanks to recent development in photographic techniques, it is possible to study the phenomenon more accurately. Lots of researches about impact dynamics and experiments on solid surfaces have been reported in the last decades.[4–7]

Surface topography plays a dominant role during the liquid droplet impact on a solid surface. For example, droplet impact on a lotus leaf which is comprised of micro-spherical bumps on the surface, will splash, leaving little liquid on the lotus leaf.[8,9] Inspired by this property, studies of droplets impact on solid surfaces with different roughness have been reported.[10–12] Different droplet behaviors on these surfaces were found out to be related to the contact angle, contact line, and roughness. Xu[13] observed this phenomenon and suggested the surface topography was an important parameter for impact droplets to prompt splash. Kannan and Sivakumar[14] investigated the droplet impact process on a hydrophobic surface which was comprised of parallel micro-grooves. They found that the groove structure changes the shape of the liquid lamella spreading on the grooved surface. Lee *et al.*[15] also recorded the dynamics of a liquid droplet that impacts on a solid surface whose wettability is patterned on the micro-scale. It has been shown that the wettability of the micro-pattern affects the impact outcomes of impinging liquid droplets. The maximum spreading diameter was derived in their study. Up to now, most reports on the impact behavior are restricted to observing the phenomenon, describing the process or deriving the functions to predict maximum spreading diameters. However, published studies on the impact of inertia dominated liquid droplets on model rough surfaces are very limited currently, such as how the micro-scale affects the impact process, what are the spreading behaviors on different micro-scaled surfaces and so on.

In this paper, the impact behaviors on different micro-patterned surfaces are considered experimentally. The maximum spreading diameters on different micro-scaled surfaces are given and fingers which are presented after impact are analyzed. The impact process is explained by the wettability of surface in different directions in the end.

2. Materials and methods

2.1. Target surfaces

Finely polished copper plate surfaces are used to prepare the target surfaces, using Quasi-LIGA molding technology. The technological sketch of the target surfaces used in the present study is shown in Fig. 1. The target surfaces are patterned into micro-grooved spokes that radiate from the center, concentric circles, and parallel lines on the polishing copper plate, and shown in Fig. 2. In the present study, major geometrical dimensions of the grooved surface, groove width, l, and groove depth, h, are kept at 0.2 mm and 0.2 mm, respectively.

*Project supported by the National Natural Science Foundation of China (Grant No. 51109178) and the Science and Technology Innovation Foundation of Northwestern Polytechnical University, China (Grant No. JC20120218).

†Corresponding author. E-mail: huhaibao@nwpu.edu.cn

© 2013 Chinese Physical Society and IOP Publishing Ltd

For the parallel micro-grooved surface, the width of solid pillar which separates any two successive grooves, s, is kept at 0.2 mm. For the micro-patterned surfaces, all the micro-grooves are well-distributed on the limited area (2 cm×2 cm).

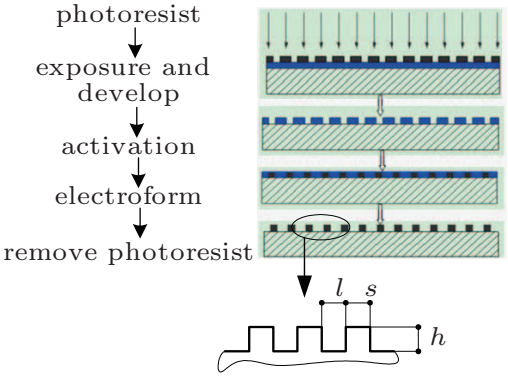


Fig. 1. (color online) Technological sketch of the target surfaces.

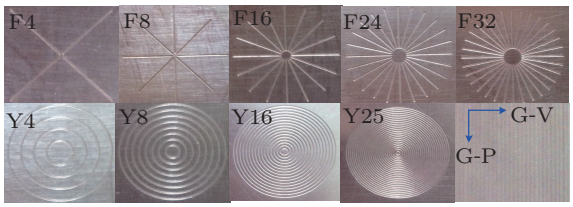


Fig. 2. (color online) Images of the target surfaces.

The radiant patterned target surface is signified by FN, in which F denotes the radiant form of the pattern and N represents the number of the spokes. The circular patterned target surface is signified by YN in which Y denotes the circular shape of the pattern and N represents the number of the rings. In the experiment, the number of the micro-grooves for the radiant shape changes from 4 to 32 while the number of the rings varies from 4 to 25. The target surface which has parallel micro-grooves is signified by G-P and G-V here in which P denotes the parallel direction and V refers to the vertical direction of the micro-groove. Impact experiments on the smooth surface are examined to describe the role played by surface grooves of the grooved surface in droplet impact process which is denoted by S here.

2.2. Experimental method

The apparatus used in this experiment is shown schematically in Fig. 3. A photographic technique is employed to capture the physical events occurring during droplet impact process. A CCD camera (RED LAKE, IDT N4) is positioned above the target surfaces to capture the entire event of droplet motion at 3000 frames per second. The pictures of experiment are treated by Image-ProPlus. For the droplet, distilled water with density $\rho = 996$ kg/m^3, surface tension $\sigma = 0.07275$ N/m, and viscosity $\mu = 0.001$ kg/ms is used in the experiment.

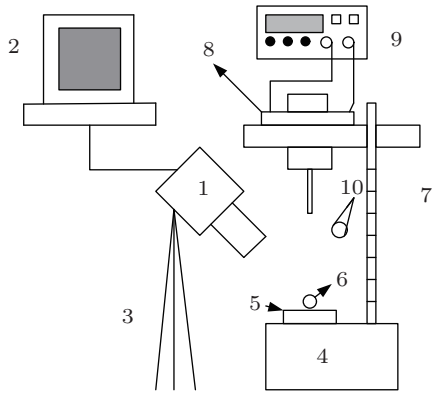


Fig. 3. Schematic diagram of the experimental setup. 1: high-speed camera, 2: PC, 3: tripod, 4: table, 5: target surface, 6: droplet, 7: guide rail, 8: droplet generator, 9: current source, 10: lamp-house.

In the experiment, droplet is generated by the liquid drop generator with constant volume. So the radius of the droplet is kept at 1.5 mm. The impact velocity is dominated by the distance between the generator and the surface. Then the impact velocity can be obtained from two successive pictures just before impacting. Five kinds of impact velocities are discussed in our study: 1.33 m/s, 1.83 m/s, 2.33 m/s, 2.67 m/s, 3.17 m/s, which are corresponding to five kinds of Weber numbers: 72.8, 137.8, 223.4, 293.4, 413.6.

3. Results and discussion

3.1. Spreading and recoiling of liquid drops

Figure 4 shows some image sequences of droplet spreading process on the micro-grooved surface for different values of Weber number. The temporal measurements of impact ratio β, obtained during the impact of liquid drops with different values of Weber number on the target surfaces, are given in Fig. 5. The spreading ratio β is defined as $\beta = D_C/D_0$, where D_C is the instantaneous contact radius and D_0 is the radius of the droplet.

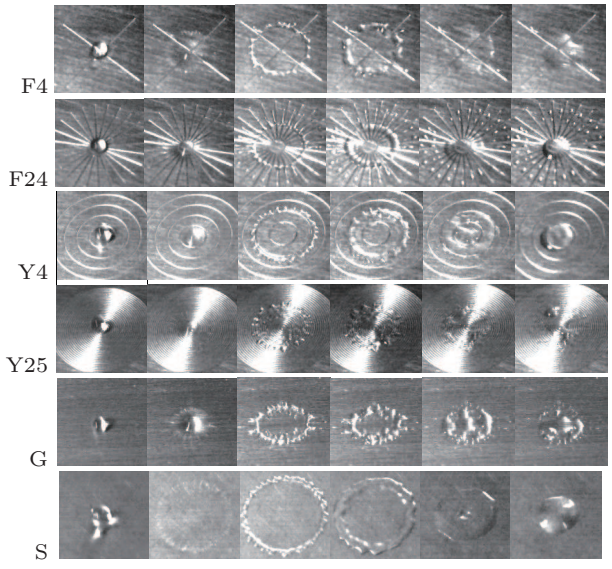


Fig. 4. Image sequences of the droplet spreading process.

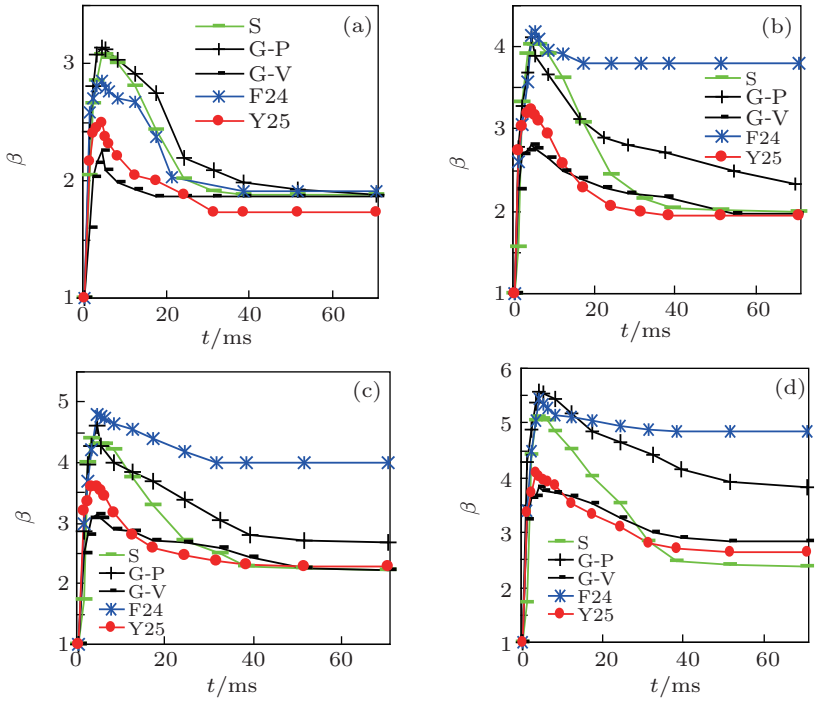


Fig. 5. (color online) Variations of normalized spreading drop diameter with time in the spreading process: (a) $We = 72.8$, (b) $We = 137.8$, (c) $We = 223.4$, and (d) $We = 413.6$.

Based on the images recorded, it can be found that the impact processes on the radiant patterned, circular patterned, and parallel micro-grooved surfaces include spreading and recoiling process just like those on the polished surface. But due to different distributions of the micro-grooves, lots of different impact behaviors are obtained on different micro-patterned surfaces which are given as follows.

(i) At lower impact velocity (Weber number = 72.8), the spreading processes are arrested on the surfaces which have micro-patterns. On the parallel micro-grooved surface, the spreading velocity in the direction along the groove direction is faster than that in the direction perpendicular to the groove direction. So the groove structure changes the spread velocity which results in elliptical lamella after impact on the polished surface rather than circular lamella. It can be inferred that some portion of liquid permeates into the grooves at lower velocity which magnifies the viscid drag so the spreading diameter on micro-patterned surface is smaller than that on the polished surface.

(ii) As the increase of impact velocity (Weber number values are 137.8, 223.4, and 413.6), different micro-patterned surfaces influence the spreading process more and more obviously. The radiant patterns conduct the spreading process while circular patterns hinder it. At higher impact velocity, the grooves on the micro-patterned surface lead to the spreading direction of liquid just like a function of rail. Because of this, the droplet liquid flowing along the grooves shows more perturbations even is ejected out during spreading process while some fingers appear at the same time. For the circular patterned surfaces, it hinders the spreading just like a pit because of the increased viscid drag.

(iii) Considering the recoiling process at low velocity (Weber number = 72.8), the final states of all the target surfaces are alike each other basically. It can be explained as follows: as the low inertia, the area of lamella is so small that the energy stored in the droplet is enough to reach the minimum energy state as shown in Fig. 6(a).

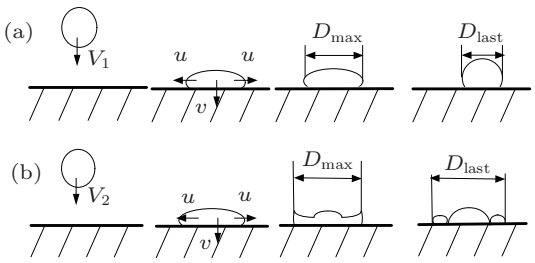


Fig. 6. Diagrammatic sketch of impact process.

(iv) As the increasing of impact velocity (Weber number values are 137.8, 223.4, and 413.6), the recoiling processes on the different micro-pattered surfaces change a lot. For the radiant patterned surfaces, the recoiling process becomes more and more weakly as the number of spokes increases. However, for the circular patterned surfaces, the recoiling process exist all the times. The recoiling process in the direction along the groove direction is stronger than that in the direction perpendicular to the groove direction, which occurs on the parallel micro-grooved surface. The mechanisms of these processes

are shown in Fig. 6(b). When the spreading radius reaches the critical dimension, the lamella develops a depression because of the spreading, so the fraction of droplet liquid cannot be held by the surface tension, even broken into tiny droplets which result in a weak or no retraction.

3.2. Maximum spread diameters

Figure 7 shows image sequences of the spreading process of impacting liquid drops which reach maximum spread diameters on the micro-grooved surfaces in different values of Weber numbers. It can be found that the maximum spread diameters on the target surfaces increase with the Weber number increasing. For some surfaces such as F16, F32, and G-P, the maximum spread diameters are even larger than those for the polished surface. The maximum spread diameters change on the different micro-patterned surfaces with the same Weber number. The results are shown in Fig. 8. For the radiant patterned surfaces, the spreading ratio β increases with the value of N increasing. However, the spreading ratio β decreases with the value of N increasing on the circular patterned surfaces. For the parallel micro-grooved surface, the droplet develops an instantaneous ellipsoid-shaped lamella as seen in Fig. 7. It can be further inferred that the micro-pattern hinders the spreading process at low impact velocity. But as the impact velocity increases, micro-grooves which are parallel to the spreading direction conduct the spreading process while the perpendicular micro-grooves hinder it.

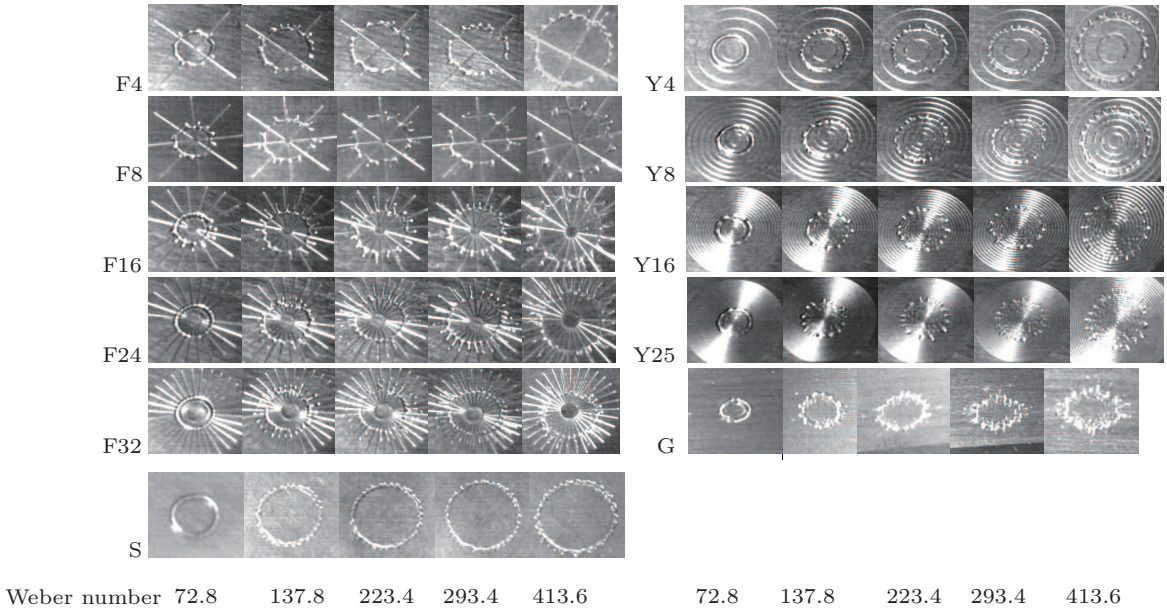


Fig. 7. Images of droplets impacting with various values of Weber number on the target surfaces at the maximal spreading.

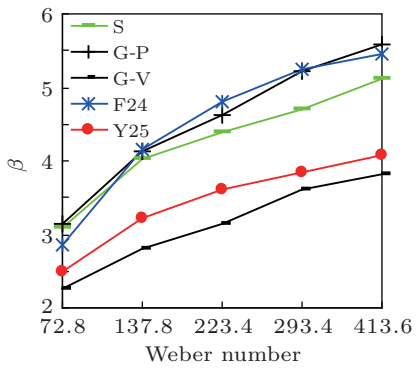


Fig. 8. (color online) Variations of β with impact Weber number.

3.3. Attendant fingers

The micro-pattern may induce corrugations of the rims in the spreading stages which can be observed in Fig. 7. The rims of spreading droplets formed by the impact of a droplet onto a solid surface at high Weber number are known to develop an instability, which is termed fingering.[15] This fingering is observed on all the surfaces at large values of Weber number. It can be found that the micro-pattern influences the length and number of fingers. Therefore, the numbers and dimensions of fingers formed by collision on the micro-patterned surfaces when the lamella reaches maximum spreading diameters are measured. The results are shown in Figs. 9 and 10, respectively. Letter N represents the number of fingers in Fig. 9.

It can be found from Fig. 9 that fingers exist on all the surfaces at higher values of Weber number while only the fingers with small values of N, 4–16, at lower values of Weber number, exist on radiant patterned surfaces. For the radiant patterned surfaces, the number of fingers which are located

near the grooves is equal to the number of spokes at higher values of Weber number approximately. But for the circular patterned surfaces, their numbers of fingers are close to each other. However, most fingers exist on the polished surface, which is different from previous study.[14,15] Besides, the droplet liquid will be ejected out as tiny droplets go beyond the micro-patterned area when the value of Weber number is large enough as shown in Fig. 7.

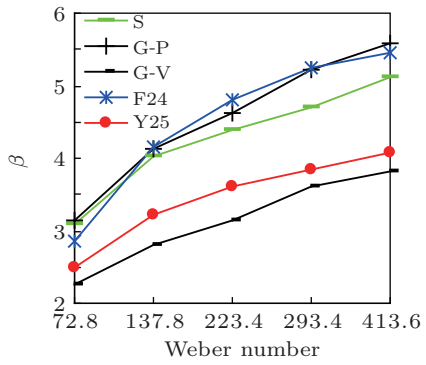


Fig. 9. (color online) Variations of finger number with impact Weber number.

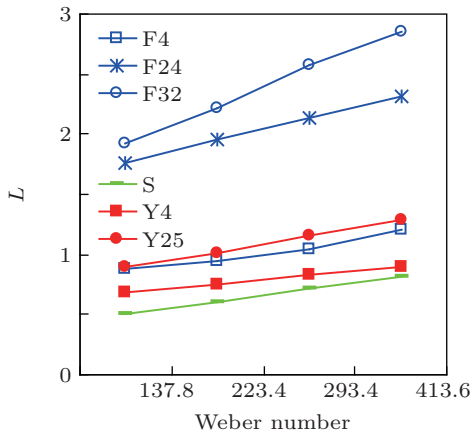


Fig. 10. (color online) Dependences of the length of finger on Weber number.

The lengths of fingers increase with the value of Weber number increasing on all the surfaces. Fingers on the radiant patterned surfaces are longest while on the polished surface, shortest. This phenomenon will be more obvious with the number of spokes increasing. For the circular patterned surfaces, the lengths of fingers change faintly as the number of rings increases. The shapes of fingers on the radiant patterned surfaces are long and thin while short and wide on the circular patterned surfaces. Thus, micro-grooves which are parallel to spreading direction induce that fingers to spread along the grooves rapidly.

3.4. Theoretical analysis of maximum spread diameter

From Ref. [16] the equation about the maximum spread diameter on the polished surface is

$$\beta = \frac{D_C}{D_0} = \sqrt{\frac{We+12}{3(1-\cos\theta)+4(We/\sqrt{Re})}}, \quad (1)$$

where We is the Weber number. It can be seen from Eq. (1) that the contact angle can influence maximum spread diameter. The spreading ratio β decreases as contact angle increases.

The micro-grooved surface has different values of wettability in different directions (as shown in Fig. 11). This phenomenon obtained on the grooved surface is in qualitative agreement with the previous work.[17] The contact angle is small on the surface perpendicular to the groove direction while large on the surface parallel to the groove direction. So the maximum spread diameter is longer in the direction which is parallel to the groove.

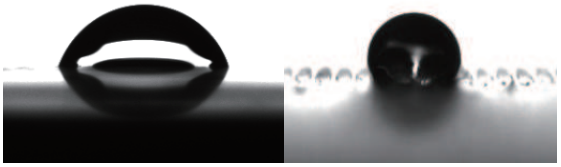


Fig. 11. Representative images of water droplets residing on micro-grooved surface.

In the experiment, the radiant pattern acts just like the parallel micro-grooves while the circular pattern acts like the perpendicular micro-grooves. Because of this, spread diameter on the radiant patterned surface is longer, which coincides with the experimental result.

4. Conclusions

It has been shown that the dynamics of a liquid drop impacting on a solid surface is greatly influenced by different micro-patterns on the target surface. These effects exist in the spreading stages and recoiling stages. A systematic comparison between the experimental results of drop impact on the micro-grooved surface and those obtained on the polished surface reveals the following outcomes.

The geometry of groove structure governs the spreading process of impact droplets on the grooved surface. For the droplets at lower velocity, the micro-patterned surface hinders the spreading of droplet liquid. But as impact velocity increases, the radiant patterns conduct the spreading process while the circular patterns hinder it. On the micro-grooved surface, the droplet spreads faster in the direction along the groove direction than in the direction perpendicular to the groove direction. Because of this, an elliptical-shaped lamella develops on the parallel micro-grooved surface.

The radiant patterned surface influences the recoiling process by forming long fingers around the edges of the lamella. But for the circular patterned surface, the droplet recoils show

more or less similar trends as seen with the polished surface. This phenomenon is more obvious at a higher impact velocity.

The number and sizes of fingers on a micro-patterned surface are different from those naturally occurring on a polished surface. The radiant patterned surface changes the number and sizes of fingers on which fingers are longer and thinner than on the other surfaces. However, on the circular patterned surface the number of fingers are reduced and the fingers are shorter and wider than on the polished surface.

References

[1] Worthington A M 1877 *Proc. R. Soc. Lond. A* **25** 261
[2] Yarin A L 2006 *Ann. Rev. Fluid Mech.* **38** 159
[3] Deegan R D, Brunet P and Eggers J 2008 *Nonlinearity* **21** 1
[4] Li X Y, Ma X H and Lan Z 2010 *Langmuir* **26** 4831
[5] Moita S and Moreira L 2007 *Int. J. Heat Fluid Flow* **28** 735
[6] Guo J, Dai S Q, Dai Q 2010 *Acta Phys. Sin.* **59** 2601 (in Chinese)
[7] Bi F F, Guo Y L, Shen S Q, Chen J X and Li Y Q 2012 *Acta Phys. Sin.* **61** 184702 (in Chinese)
[8] Barthlott W and Neinhuis C 1997 *Planta* **202** 1
[9] Feng L, Li S H, Li Y S, Li H J, Zhang L J, Zhai J, Song Y L, Liu B Q, Jiang L and Zhu D B 2002 *Adv. Mater.* **14** 1857
[10] Merlen A and Brunet P 2009 *J. Bionic Eng.* **6** 330
[11] Rioboo R, Marengo M and Tropea C 2002 *Exp. Fluids* **33** 112
[12] Samuel L, Manzello and Jiann C Y 2003 *Phys. Fluids* **15** 257
[13] Xu L 2007 *Phys. Rev. E* **75** 056316
[14] Kannan R and Sivakumar D 2008 *Colloid Surface A* **317** 694
[15] Minhee L, Young S C and Ho Y K 2010 *Phys. Fluids* **22** 072101
[16] Pasandideh-Fard M, Qiao Y M, Chandra S and Mostaghimi J 1996 *Phys. Fluids* **8** 650
[17] Chen Y, He B, Lee J and Patankar N A 2005 *J. Colloid Interf. Sci.* **281** 458